



[Ru(bpy)₃]²⁺-functionalized polydopamine-coated polyurethane foam as an easily reusable macroscopic heterogeneous catalyst for visible-light photocatalysis

Han Peng, Thierry Romero, Vasiliki Papaefthimiou, Philippe Bertani, Vincent Ritleng

► To cite this version:

Han Peng, Thierry Romero, Vasiliki Papaefthimiou, Philippe Bertani, Vincent Ritleng. [Ru(bpy)₃]²⁺-functionalized polydopamine-coated polyurethane foam as an easily reusable macroscopic heterogeneous catalyst for visible-light photocatalysis. *Molecular Catalysis*, 2023, 545, pp.113183. 10.1016/j.mcat.2023.113183 . hal-04200307

HAL Id: hal-04200307

<https://hal.science/hal-04200307>

Submitted on 8 Sep 2023

HAL is a multi-disciplinary open access archive for the deposit and dissemination of scientific research documents, whether they are published or not. The documents may come from teaching and research institutions in France or abroad, or from public or private research centers.

L'archive ouverte pluridisciplinaire **HAL**, est destinée au dépôt et à la diffusion de documents scientifiques de niveau recherche, publiés ou non, émanant des établissements d'enseignement et de recherche français ou étrangers, des laboratoires publics ou privés.

[Ru(bpy)₃]²⁺-functionalized polydopamine-coated polyurethane foam as an easily reusable macroscopic heterogeneous catalyst for visible-light photocatalysis

Han Peng,^a Thierry Romero,^b Vasiliki Papaefthimiou,^b Philippe Bertani,^c Vincent Ritleng^{a,*}

a Université de Strasbourg, Ecole européenne de Chimie, Polymères et Matériaux, CNRS, LIMA, UMR 7042, 25 rue Becquerel, 67087 Strasbourg, France. vritleng@unistra.fr

b Université de Strasbourg, Ecole européenne de Chimie, Polymères et Matériaux, CNRS, ICPEES, UMR 7515, 25 rue Becquerel, 67087 Strasbourg, France

c Université de Strasbourg, CNRS, Institut de Chimie, UMR 7177, 4 rue Blaise Pascal, 67081 Strasbourg, France

Abstract

An easy-to-handle, highly reusable and efficient [Ru(bpy)₃]²⁺-based heterogeneous photocatalyst was obtained by post-functionalization of a polydopamine-coated open cell polyurethane foam (PDA@PUF) via a silanization process of the mussel-inspired adhesive layer with 3-(triethoxysilyl)propan-1-amine (APTES), followed by an EDC-mediated coupling with [2,2'-bipyridine]-4-carboxylic acid and further complexation with [Ru(bpy)₃Cl₂] (bpy = 2,2'-bipyridine). The successful covalent grafting of APTES on the PDA layer of PUF and functionalization all over the foam surface with [Ru(bpy)₃]²⁺ was suggested by ²⁹Si CP-MAS NMR, XPS, ICP-AES and SEM-EDX. The macroscopic photocatalyst proved effective in model benzylic amine homocouplings and cross dehydrogenative couplings under visible-light irradiation and molecular oxygen, showing

good functional group tolerance and excellent reusability in an easy-to-carry “dip-and-play” mode for at least six runs. Impressively, an improvement of the catalytic performances was even observed in both reactions, which most likely results from a modification of the uppermost layer of polydopamine throughout the successive cycles that renders the photocatalyst more accessible.

Keywords: Visible-light photocatalysis; Polyurethane open cell foams; Polydopamine; Ruthenium; Oxidative benzylic amine homocoupling; Cross dehydrogenative coupling.

1. Introduction

Structured catalytic supports (SCS) provide large surface-to-volume ratios, efficient mass transfers and small pressure drop. Their open structure along with their macroscopic shape allow an intimate mixing of the reagents, as well as an easy accessibility of the reactants to the active sites, while avoiding a tedious separation of the products from the catalyst [1]. These properties largely benefit the industry in continuous processes. Among the variety of SCSs, open cell foams account for a large proportion. Metallic and ceramic foams, in particular, are prime candidates as host supports for catalytically active metallic nanoparticles (NPs) [2,3,4]. Their preparation however comprises multiple steps, including high-temperature processes for the production of the macroscopic host structures, as well as energy intensive processes for the deposition and activation of the catalytic phase on the support surface, such as the calcination and reduction steps [3]. In addition, these foams display many disadvantages: (i) their rigid structures make them easily breakable, (ii) the presence of randomly distributed closed cells renders the reproducibility of reactions uncertain, and (iii) the recovery of the catalyst adsorbed on the foam often necessitates numerous chemical treatments in highly corrosive media before landfill disposal [5].

Due to their commercial availability, low price, interesting mechanical properties and easiness of engineering, open cell polyurethane foams (PUF) represent an interesting alternative [6] that perfectly compensates for the above described drawbacks of ceramic and metallic foams. However, finding a way to deposit an active phase without altering their mechanical and transport properties was a critical issue as PUFs are devoid of microporosity. Inspired by the mussel-like adhesive principle [7], our group successfully coated PUFs with an thin adhesive layer of polydopamine (PDA) by a simple dipping method in a buffered (pH 8.5) aqueous solution of dopamine [8] and applied the resulting PDA@PUF structure support in dye removal [9,10,11] or catalysis [12,13,14,15] processes after further functionalization with metal [10,13,15] or metal oxide [9,14] nanoparticles, molecular catalysts [12,16], or hydrides [10,11]. The strong adhesive properties of the PDA layer, inferred by an array of interactions going from weak forces to covalent bonds [17], ensured both a robust coating of the PUF materials and a robust anchoring of the active phase, whatever its nature, and thus minimal leaching into the reaction medium. This property together with the “dip-and-play” characteristics of the PDA@PUF macroscopic support resulted in easily reusable catalysts [8-16]. In particular, TiO₂-functionalized PDA@PUF foams proved highly efficient and reusable for the photodegradation, under UV irradiation, of acid orange 7 [9] and formic acid in water [14], and of volatile organic compounds in air [14].

Visible-light photoredox catalysis, as a powerful and effective tool in organic synthesis, has become a prominent topic through single-electron or energy transfer processes under mild reaction conditions [18,19]. In particular, [Ru(bpy)₃]²⁺ – with or without a co-catalyst merger – has shown its applicability in a myriad of visible-light-induced reactions including, among others, reductive dehalogenations [20], amine functionalizations [21], hydroxylation of arylboronic acids [22], cycloadditions [23,24,25,26,27], cross dehydrogenative couplings [28,29], base-free cross-couplings of ammonium alkylsilicates [30], photoinduced electron

transfer–reversible addition–fragmentation chain transfer (PET-RAFT) polymerizations [31,32] or asymmetric α -functionalizations of aldehydes [33,34]. Despite this impressive versatility, important limitations arise from the high cost and toxicity of ruthenium, as well as the high molar extinction coefficient of $[\text{Ru}(\text{bpy})_3]^{2+}$ that hampers light penetration into the solution and causes dramatically reduced reaction rates when scaling-up reactions in traditional batch reactors due to the low surface area to volume ratio of the latter [35]. Possible answers to these limitations go through the immobilisation of the photocatalyst (PC) on a solid support, its incorporation in supramolecular systems, or its transformation into amphiphilic or other specific derivatives compatible with liquid–liquid phase-separation, to develop easily recoverable and reusable heterogeneous visible-light PCs [36], and/or the use of continuous flow reactors [37].

Immobilized catalytic systems may additionally allow (i) a better control of the reaction efficiency and selectivity through the tuning of the environment in the vicinity of the photocatalytic centres, (ii) an improvement of the photostability of the PCs and a decrease of self-quenching processes through functionalization of the photosensitizer and spatial separation of the catalytic centres, and (iii) the use in solvents where the PCs are insoluble or inactive. In terms of host matrix, a vast array of strategies has been studied to immobilize $[\text{Ru}(\text{bpy})_3]^{2+}$, going from simple to sophisticated systems including, for instance, nanoporous carbon nitrides [38], reduced graphene oxide [39], anionic mesoporous metal-organic frameworks [40] or supramolecular organic frameworks [41]. Even though all these reusable heterogeneous PCs were effectively applied in various types of visible light-induced transformations, the whole processes - including the support preparation - are somewhat short of some dexterities and proceeding conveniences for scale up procedures. The expectation for more applicable heterogeneous PCs is that the building blocks should be easily obtainable at low environmental and economic cost, the preparation of the supported PC simple, and the

catalytic applications easily diversified.

Polydopamine, on the other hand, has been demonstrated to act as an efficient visible-light-harvesting material [42,43] and redox mediator [10] able to accelerate the rate of photoinduced electron transfer via a two-electron and two-proton redox-coupling mechanism [44]; two properties that can clearly be beneficial in heterogeneously photocatalyzed processes [45,46,47,48,49].

In this context, we report here our studies toward the immobilisation of $[\text{Ru}(\text{bpy})_3]^{2+}$ on redox non-innocent, easy-to-prepare and easy-to-handle PDA-coated polyurethane foams [8-16], which furthermore possesses sufficiently large cells to allow efficient light penetration inside the whole three-dimensional structure as well as efficient transport properties under flow conditions, and which - due to its lightweight and flexibility - can be easily engineered and adapted to any kind of (photo)reactor [14].

Thanks to the presence of catechol moieties on the surface of the PDA adhesive layer, (3-aminopropyl)triethoxysilane (APTES) was readily anchored on PDA@PUF, accomplishing a surface amination allowing the subsequent grafting of the PC via EDC-mediated coupling with [2,2'-bipyridine]-4-carboxylic acid and further complexation with $[\text{Ru}(\text{bpy})_2\text{Cl}_2]$. The resulting $\text{Ru}(\text{bpy})_3\text{-APTES@PDA@PUF}$ material was characterized by a combination of ^{29}Si CP-MAS NMR and XPS spectroscopies, ICP-AES analyses, SEM microscopy and SEM-EDX elemental mapping, and its catalytic activity studied in model oxidative benzylic amine homocouplings [50,51,52,53,54,55,56,57,58] and C-H bond functionalizations of N-phenyl-tetrahydroisoquinoline [50,51,52,59, 60,61,62] under visible-light irradiation and O_2 as a green oxidant source [63]. The macroscopic catalyst proved catalytically effective in both reactions with a good functional group tolerance and showed excellent reusability for at least 6 runs in an easy-to-carry “dip-and-play” mode. Impressively, although some Ru leaching was measured, an improvement of the catalytic performances was even observed over the 6 runs

in both reactions, which most likely results from a modification of the uppermost layer of PDA that renders the $[\text{Ru}(\text{bpy})_3]^{2+}$ photocatalyst more accessible, as revealed by the progressive colour change of the catalytic foams from dark brown to dark red or orange, the smoothing of their surface, and XPS analyses.

2. Experimental Section

2.1. Materials and methods

Unless otherwise stated, all reagents and solvents were used as provided by the commercial suppliers. Polyurethane open cells foams (20 PPI, TCL 40100 soft white reticulated) were given by FoamPartner. Dopamine hydrochloride (008896), EDC hydrochloride (024810), *N*-hydroxysuccinimide (005022) and 3-aminopropyltriethoxysilane (ISI0010-98) were purchased from Fluorochem. Tris base (99.9+% - T1503), ammonium acetate ($\geq 98\%$ - A7330), 2-acetylpyridine ($\geq 99\%$ - W325104) and crotonaldehyde ($\geq 99\%$ - 262668) were purchased from Sigma-Aldrich. 4-Chlorobenzylamine (97+% - A13984), 4-*tert*-butylbenzylamine (98% - L20394) and 3-(aminomethyl)pyridine (98+% - B23634) were provided by Alfa Aesar. 4-(Trifluoromethyl)benzylamine (97% - 375830010) was purchased from Acros Organics. 4-Methoxybenzylamine ($>97.0\%$ - M0870) and 2,2'-bipyridyl ($>99.0\%$ - B0468) were provided by TCI. $\text{RuCl}_3 \cdot x\text{H}_2\text{O}$ (40-43% Ru, 99.9% Ru - 44-5880) was purchased from Strem Chemicals. $\text{Ru}(\text{bpy})_2\text{Cl}_2 \cdot 2\text{H}_2\text{O}$ [64], 2,2'-bipyridine-4-carboxylic acid [65,66] and *N*-phenyl-tetrahydroisoquinoline [67,68] were prepared according to published procedures (see the Supporting Information). 18.2 M Ω deionized water (TOC < 1 ppb), supplied by a Q20 Millipore system, was used for the preparation of aqueous solutions and washing procedures with water. Purifications by column chromatography were carried out with Macherey-Nagel silica gel 60 (0.04-0.63 mm). The RGB LED strip light (Govee, H6190) was manufactured by Shenzhen Intellirocks Tech Co. Ltd.

Scanning electron microscopy (SEM) measurements were recorded with a Hitachi SU8010 FE-SEM microscope at 3 kV at room temperature. No metallization of the samples was done, but their borders were covered with a metallic tape to evacuate the excess of charge.

Elemental mapping by scanning electron microscopy-energy dispersive X-ray spectroscopy (SEM-EDX) was investigated with a Zeiss Gemini SEM 500 FEG EDAX Octane Elite EDX detector. The X-rays emitted upon electron irradiation were acquired in the range 0–20 keV. Quantification was done using the standard-less ZAF correction method in the Team EDS software from EDAX.

X-ray Photoelectron Spectroscopy (XPS) was carried out in an ultrahigh vacuum (UHV) spectrometer equipped with a RESOLVE 120 MCD5 hemispherical electron analyzer and a dual anode source (Mg/Al). For the XPS measurements, the $\text{AlK}\alpha$ line at 1486.6 eV was used. Survey and high-resolution spectra were recorded in constant pass energy mode (100 and 20 eV, respectively). Binding energies were calibrated by referring to the C1s peak at 284.5 eV. Shirley-type background subtraction and fitting of the spectra were done with the software package Casa XPS *vs.* 2.3.

Inductively coupled plasma-atomic emission spectrometry (ICP-AES) measurements were performed by the Plateforme Analytique des Inorganiques of the Institut Pluridisciplinaire Hubert Curien (UMR CNRS 7178), Strasbourg, France. For Si and Ru loading determination, $\text{Ru}(\text{bpy})_3\text{-APTES@PDA@PUF}$ samples were mineralized with aqua regia (2 mL HCl , 1 mL HNO_3) at 185 °C for 50 min under pressure (Multiwave ECO, Anton Paar). A blank test was carried out in parallel under the same conditions. Quantification in the clear obtained solutions was realized by ICP-AES (Varian 720ES) at two wavelengths for each element, 245.657 nm and 267.876 nm for Ru and 250.690 nm and 251.611 nm for Si.

Gas chromatographic (GC) analyses were carried out on an Agilent 7820A instrument

equipped with a HP-1 column (30 m, 0.35 mm, 0.25 μ m), with dihydrogen as the carrier gas and tetradecane as the internal standard. The retention times and GC responses in terms of areas versus concentrations of the reagents and products were calibrated by using pure components diluted in an acetone solution at various concentrations. The conversion and product distribution were calculated from the GC results.

Solution NMR spectra were recorded at 298 K on a Bruker Avance III HD 400 MHz spectrometer operating at 400.13 MHz for ^1H and at 100.61 MHz for ^{13}C . The chemical shifts are referenced to the residual deuterated or ^{13}C solvent peaks. Chemical shifts (δ) and coupling constants (J) are expressed in ppm and Hz respectively (see the Supporting Information).

For solid-state NMR spectra, the foam samples were frozen into liquid N_2 and grinded. The grinded foams were then packed in 4 mm ZrO_2 rotors under air. The ^{29}Si CP-MAS experiments spectra were recorded at 298 K on a Bruker Solid State DSX 300 MHz NMR spectrometer operating at 69.66 MHz, and equipped with a Bruker 4 mm $^1\text{H}/\text{X}$ CP-MAS probe. A shaped Cross-Polarization pulse sequence with tangential modulation on both channels was used with the following parameters: the spinning speed was set to 10 kHz, the spectral width to 30 kHz, the contact time was in the range of 1 ms, the proton RF field was around 55 kHz for decoupling (using SPINAL 64 sequence) and 40 kHz for contact, with a recycle delay of 5s. The spectra were calibrated with respect an external PDMS sample (–35.1 ppm).

2.2. Open cell polyurethane foam (PUF) coating with polydopamine (PDA)

The procedure was adapted from our published procedure [8,9]. Dopamine hydrochloride (2 mg/mL) was dissolved in an aqueous solution (500 mL) of Tris base (10 mM) buffered to pH 8.5 with aqueous HCl (1 M). Four samples of PUF (*ca.* 1.5 cm \times 1.5 cm \times 3 cm) were

immersed in the stirred solution for 17 h at RT. The solution turned quickly orange, then slowly black. The resulting PDA-coated foams (PDA@PUF) were then taken out of the solution, dried in an oven at 80 °C for 1.5 h, washed in vigorously stirred water (3×10 min in 500 mL,) and dried again in an oven at 80 °C.

2.3. Functionalization of PDA@PUF with APTES

A sample of PDA@PUF (*ca.* 1.5 cm \times 1.5 cm \times 3 cm) was washed in vigorously stirred toluene (3×25 mL) at room temperature for a few minutes, and dried under vacuum prior to the functionalization.

A stirring bar and the sample of PDA@PUF were introduced in a Schlenk tube, that was then put under argon. This was followed by the additions of freshly distilled toluene (25 mL) and APTES (0.23 mL, 1 mmol). After 24 h of stirring at 70 °C, the resulting APTES-functionalized foam, APTES@PDA@PUF, was removed from the reaction medium, washed for a few minutes in vigorously stirred toluene (3×25 mL), and then dried under vacuum.

APTES@PDA@PUF was characterized by ^{29}Si CP-MAS NMR, SEM, SEM-EDX, and ICP-AES revealing a mean Si content of 3.763 ± 0.041 g/kg.

2.4. Coupling of 2,2'-bipyridine-4-carboxylic acid with APTES@PDA@PUF

A sample of APTES@PDA@PUF (*ca.* 1.5 cm \times 1.5 cm \times 3 cm) was washed for a few minutes in vigorously stirred ethanol (25 mL) at room temperature before use.

A stirring bar was introduced in a Schlenk tube. This was followed by the additions of ethanol (25 mL), 2,2'-bipyridine-4-carboxylic acid (40 mg, 0.2 mmol), *N*-hydroxysuccinimide (34 mg, 0.3 mmol) and EDC hydrochloride (0.4 mmol, 76 mg), in the indicated order. After 0.5 h, the sample of APTES@PDA@PUF was then immersed into the stirred solution for 20 h at room temperature. The resulting bipyridine-coupled foam, BPY-

APTES@PDA@PUF, was then washed in acetone (3×30 mL), water (2×30 mL) and ethanol (2×30 mL), and dried under vacuum.

BPY-APTES@PDA@PUF was characterized by SEM and ICP-AES revealing a mean Si content of 2.462 ± 0.025 g/kg.

2.5. Coordination of *cis*-[Ru(bpy)₂Cl₂] \cdot 2H₂O on BPY-APTES@PDA@PUF

A stirring bar and a sample of BPY-APTES@PDA@PUF (*ca.* 1.5 cm \times 1.5 cm \times 3 cm) were introduced in a Schlenk tube. This was followed by the successive additions of H₂O/EtOH (1:1) (25 mL) and Ru(bpy)₂Cl₂ \cdot 2H₂O (52 mg, 0.1 mmol). The reaction medium was then heated under stirring by putting the tube in an oil bath at 95 °C. After 24 h reaction, the resulting Ru-coordinated foam, Ru(bpy)₃-APTES@PDA@PUF, was removed from the solution and then rinsed with ethanol (3×30 mL), H₂O (2×30 mL), and acetonitrile (2×30 mL).

Ru(bpy)₃-APTES@PDA@PUF was characterized by SEM-EDX, XPS, and ICP-AES revealing a mean Si content of 1.564 ± 0.020 g/kg and Ru content of 2.024 ± 0.027 g/kg.

2.6. General procedure for the oxidative homocoupling of benzylic amines photocatalyzed by Ru(bpy)₃-APTES@PDA@PUF

A stirring bar and a sample of Ru(bpy)₃-APTES@PDA@PUF of *ca.* 1.5 cm \times 1.5 cm \times 3 cm, whose mass (225 mg) was adjusted in function of its Ru content established by ICP-AES (0.202 wt%) to have a Ru loading of 4.5 μ mol, were introduced in a Schlenk tube. Acetonitrile (10 mL) was then added to immerse totally the foam. This was followed by the addition of the benzylic amine (0.5 mmol). The tube was then closed with a rubber septum, its atmosphere quickly evacuated under vacuum and backfilled with O₂ several times. Under O₂, supplied by a balloon, the tube was placed under the irradiation of an 18 W LED blue

light and the mixture was stirred (1000 rpm) at room temperature for 48 h. It is noteworthy that light irradiation induced some heat aggregation around the Schlenk tube, generating an external temperature of 30-35 °C. The benzylic amine conversion to the corresponding imine was then determined by sampling the reaction medium, and analysing the removed aliquot (50 μ L) by GC or ^1H NMR. The aliquot was diluted with acetone or ethanol (3 mL) for GC analysis or dried under high vacuum and re-dissolved in a deuterated solvent for ^1H NMR spectroscopy. The reaction medium was then evaporated to dryness and the crude material purified by bulb-to-bulb distillation to give the pure product, whose identity was confirmed by ^1H and ^{13}C NMR spectroscopy.

2.7. General procedure for the cross dehydrogenative couplings photocatalyzed by $\text{Ru}(\text{bpy})_3\text{-APTES@PDA@PUF}$

A stirring bar and a sample of $\text{Ru}(\text{bpy})_3\text{-APTES@PDA@PUF}$ of *ca.* 1.5 cm \times 1.5 cm \times 3 cm, whose mass (225 mg) was adjusted in function of its Ru content established by ICP-AES (0.202 wt%) to have a Ru loading of 4.5 μmol , were introduced in a Schlenk tube. Methanol (10 mL) was then added to immerse totally the foam. This was followed by the addition of *N*-phenyl-tetrahydroisoquinoline (21 mg, 0.1 mmol) and of the nucleophile (2 mmol). The tube was then closed with a rubber septum, its atmosphere quickly evacuated under vacuum and backfilled with O_2 several times. Under O_2 , supplied by a balloon, the tube was placed under the irradiation of an 18 W LED blue light and the mixture was stirred (1000 rpm) at room temperature for 24 h. It is noteworthy that light irradiation induced some heat aggregation around the Schlenk tube, generating an external temperature of 30-35 °C. At the end of the reaction, the catalytic foam was removed from the medium and rinsed with ethyl acetate (2 \times 10 mL). The washing liquors were added to the medium and all the solvents evaporated under vacuum. The crude material was subsequently purified by column

chromatography over silica using petroleum ether/ethyl acetate (10:1) as eluent to give the pure desired product, whose identity was confirmed by ^1H and ^{13}C NMR spectroscopy.

2.8. Ru(bpy)₃-APTES@PDA@PUF recovery and reuse in successive photocatalytic experiments

The above-described general procedures for the photocatalytic benzylamine oxidative couplings and cross dehydrogenative couplings (CDC) were followed using benzylamine (55 μL , 0.5 mmol) for the oxidative homocouplings, *N*-phenyl-tetrahydroisoquinoline (21 mg, 0.1 mmol) and nitromethane (107 μL , 2 mmol) for the CDC, and an as-synthesized sample of Ru(bpy)₃-APTES@PDA@PUF of *ca.* 1.5 cm \times 1.5 cm \times 3 cm (225 mg, 0.202 wt% Ru, *i.e.*: $4.5 \cdot 10^{-3}$ mmol) as catalyst for each reaction type. After each photocatalytic run, the Ru(bpy)₃-APTES@PDA@PUF foam was removed from the reaction medium, washed by immersing it successively in acetone (3 \times 15 mL) and H₂O (3 \times 15 mL) for 30 min under sonication each time, and then dried under vacuum.

2.9. Ru leaching influence on the course of a photocatalytic process

In this control experiment aiming at evaluating the influence of ruthenium leaching on the reaction progress of a cross dehydrogenative coupling, the above-described general procedure was followed using *N*-phenyl-tetrahydroisoquinoline (21 mg, 0.1 mmol), nitromethane (107 μL , 2 mmol), and a sample of as-synthesized Ru(bpy)₃-APTES@PDA@PUF of *ca.* 1.5 cm \times 1.5 cm \times 3 cm (225 mg, 0.202 wt% Ru, *i.e.*: $4.5 \cdot 10^{-3}$ mmol) as catalyst, excepted that, after 8 h reaction, an aliquot (50 μL) of the medium was removed to monitor the progress of the reaction by ^1H NMR and 10 mL of methanol was added to the medium. The reaction medium was then immediately split into two equal portions of 10 mL - one with the photocatalytic foam and the other without the foam - that

were each allowed to continue to react under similar conditions (*ca.* 30-35 °C, O₂, 18W LED blue light). After 16 h more, the courses of both the blank and foam-catalysed reactions were monitored by removing aliquots (50 µL) and analysing them by ¹H NMR.

3. Results and discussion

3.1. Preparation and characterization of Ru(bpy)₃-APTES@PDA@PUF

The chosen strategy for the immobilization of [Ru(bpy)₃]Cl₂ at the surface of polydopamine-coated open cell polyurethane foams (PDA@PUF) relies on the previously-established proof of concept regarding the feasibility to covalently graft a molecular catalyst bearing an alkoxysilyl arm by condensation of the latter with the catechol groups of the mussel-inspired layer [12]. Thus, after coating a cubic sample of PUF of *ca.* 1.5 cm × 1.5 cm × 3 cm with a thin layer of PDA by simple immersion in an aqueous solution of dopamine at room temperature buffered at a pH of 8.5, close to that of a marine environment, and several washings with water [8,9], the resulting PDA@PUF material was functionalized with [Ru(bpy)₃]Cl₂ in three steps via (i) a silanization process with 3-(triethoxysilyl)propan-1-amine (APTES), (ii) the EDC-mediated coupling of [2,2'-bipyridine]-4-carboxylic acid with the resulting amino-functionalized foam, and (iii) the complexation of ruthenium to the anchored bipyridine units by reaction with *cis*-[Ru(bpy)₂Cl₂] (Fig. 1).

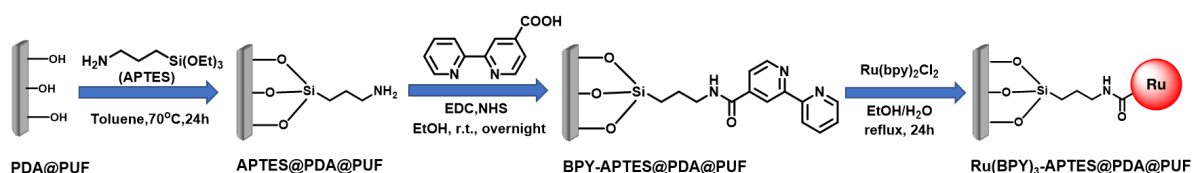


Figure 1. Functionalization strategy of PDA@PUF for the immobilization of Ru(bpy)₃²⁺

Specifically, the silanization of PDA@PUF was conducted with APTES in toluene at

70 °C for 24 h (Fig. 1). The successful covalent anchoring of APTES on the foam surface was established by ^{29}Si CP-MAS NMR spectroscopy. The NMR spectrum indeed revealed signals at -64.3 ppm, -56.4 ppm, -53.4 ppm and -42.0 ppm (Fig. 2), demonstrating the presence of T_1 , T_2 as well as cross-linked $\text{T}_3+\text{T}'_3$ and $\text{T}_4+\text{T}'_4$ substructures [69] similarly to what can be observed with covalently anchored APTES on a silica matrix [70]. In addition, ICP-AES measurements on several samples of APTES@PDA@PUF revealed a mean Si content of 3.763 ± 0.041 g/kg, and high magnification SEM images showed a rough surface characteristic of the PDA coating on PUF (Fig. S1) [9,12]. Finally, SEM-EDX spectroscopy suggested a relatively homogeneous distribution of Si on the surface of APTES@PDA@PUF as expected (Fig. S2).

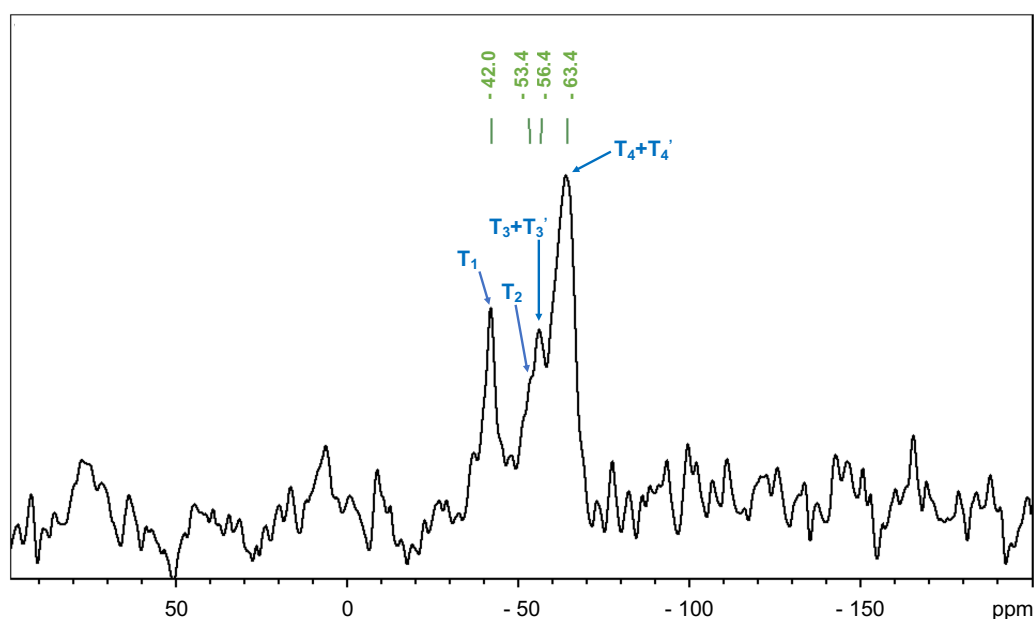


Figure 2. ^{29}Si CP-MAS NMR spectrum of APTES@PDA@PUF

After this silanization step, the primary amine groups of APTES present on the foam surface were reacted with 2,2'-bipyridine-4-carboxylic acid under EDC activating conditions in ethanol at room temperature to furnish the bpy-functionalized foam, BPY-APTES@PDA@PUF (Fig. 1). SEM images confirmed the integrity of the foam with the

absence of apparent modification of the surface (Fig. S3) and ICP-AES the preservation of the silicon anchor, though the mean Si content diminished to 2.462 ± 0.025 g/kg, most likely in reason of some cross-linked silicon crust losses.

The subsequent coordination of $[\text{Ru}(\text{bpy})_2\text{Cl}_2]$ on BPY-APTES@PDA@PUF was conducted in a hydro-alcoholic solution at 95 °C for 24 h. The black colour of BPY-APTES@PDA@PUF turned dark brown, suggesting a modification of the foam surface and the probable successful coordination of the $\text{Ru}(\text{bpy})_2^{2+}$ moiety to the anchored 2,2'-bipyridine units. Accordingly, ICP-AES measurements on several samples of $\text{Ru}(\text{bpy})_3$ -APTES@PDA@PUF revealed a mean Ru content of 2.024 ± 0.027 g/kg as well as a Si content of 1.564 ± 0.020 g/kg. Low magnification SEM images revealed a slight corrugation of the struts' edges, as was observed previously for other PDA@PUF foams, functionalized by a molecular catalyst via an analogous silanization process [12]. Higher magnification images showed a rough film structure with numerous scattered PDA aggregates, typical of PDA coating on a PUF [9,12], similarly to what was observed on APTES@PDA@PUF and BPY-APTES@PDA@PUF foams (Fig. 3). SEM micrographs combined to EDX spectroscopy revealed a relatively homogeneous distribution of C, N, O, Si and Ru over the foam surface, without apparent aggregates or segregations area, ensuring a good structural homogeneity of the material as well as a homogeneous distribution of the photocatalyst (Fig. 4, S4 and S5).

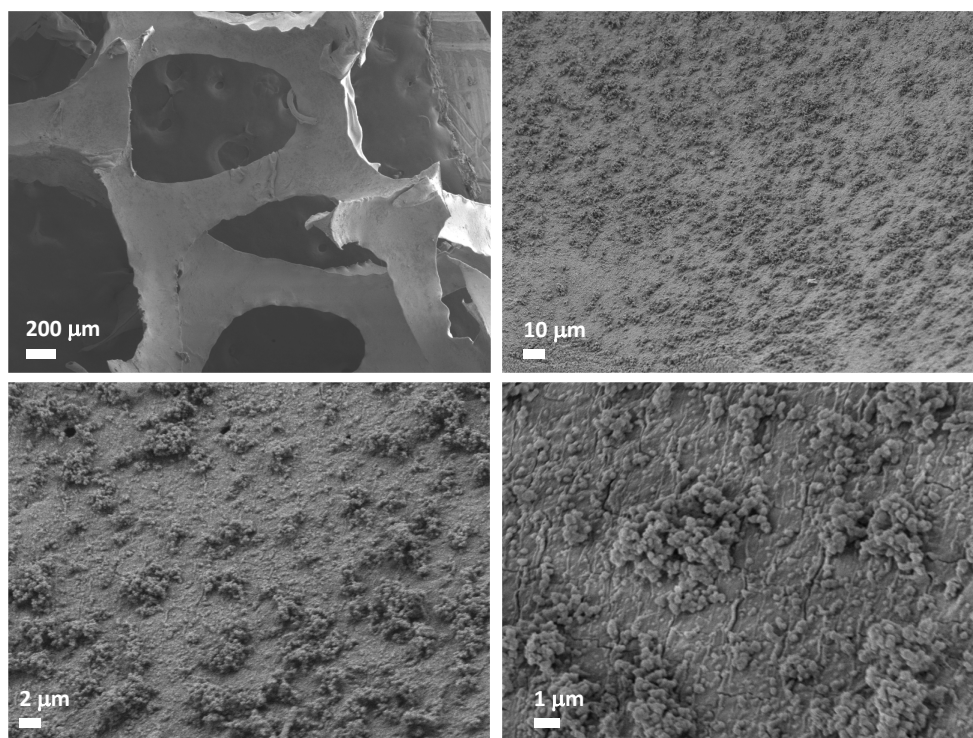


Figure 3. SEM images of as-synthesized $\text{Ru(bpy)}_3\text{-APTES@PDA@PUF}$ with different magnifications.

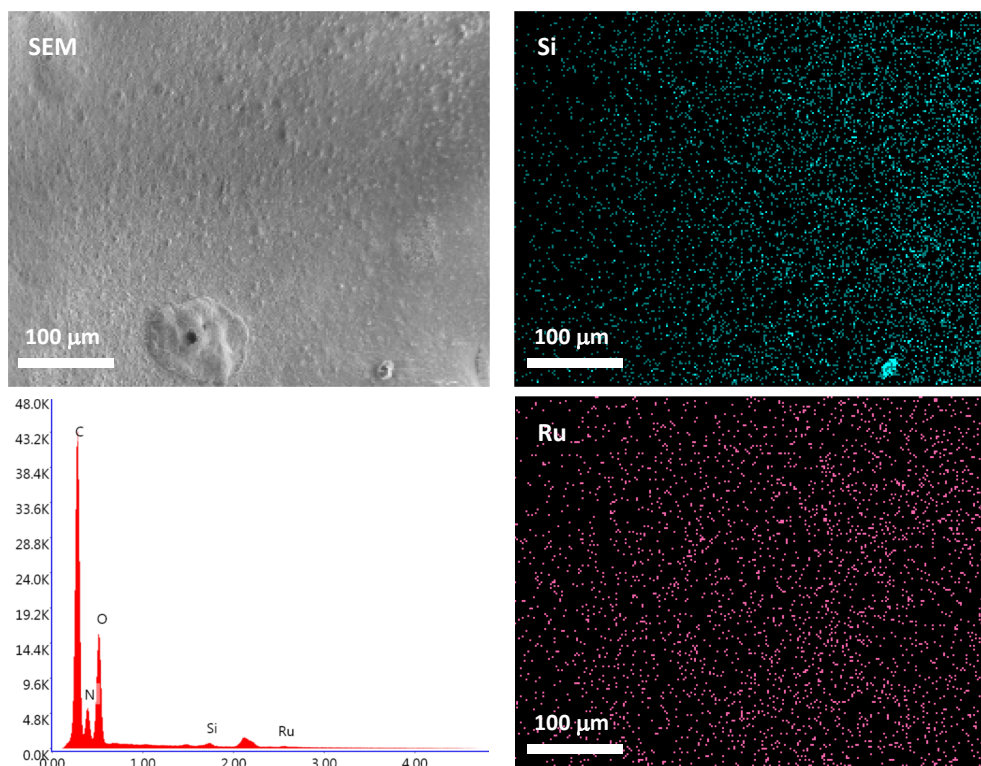


Figure 4. Elemental mapping of Si and Ru obtained by SEM-EDX spectroscopy on as-synthesized $\text{Ru(bpy)}_3\text{-APTES@PDA@PUF}$ and corresponding EDX spectrum.

X-ray photoelectron spectroscopy (XPS) was performed to gain further information about the chemical composition at the topmost surface (*ca.* 10 nm) of Ru(bpy)₃-APTES@PDA@PUF. In agreement with the result of the EDX spectroscopy, the XPS survey scan and high-resolution spectra revealed the core levels of O1s, N1s, C1s, Si2p and Ru3d elements (Fig. S6A, S7). Unfortunately, the Ru3d_{5/2} peak component has a weak signal-to-noise ratio and the Ru3d_{3/2} one overlaps with the C1s peak (Fig. S7), therefore rendering assignment to a specific ruthenium species and/or oxidation state difficult [71].

3.2. Photocatalytic activity of Ru(bpy)₃-APTES@PDA@PUF

As electrophilic intermediates, imines play a crucial role in the preparation of pharmaceuticals, pesticides and fine chemicals [72,73]. A strong stoichiometric oxidant such as 2-iodoxybenzoic acid or *N*-tert-butylbenzene-sulfinimidoyl chloride is usually required for their preparation from amines. Recently, however, efforts have been devoted to the development of heterogeneous visible-light photocatalysts for these transformations [63]. In particular, immobilized transition metal complexes have been studied to develop functional group-tolerant photocatalytic processes, using O₂ as the oxidant [36]. Herein, Ru(bpy)₃-APTES@PDA@PUF catalyst was thoroughly investigated in visible-light-induced oxidative couplings of benzylic amines under mild conditions (.

Initial studies focused on the oxidative homocoupling of benzylamine under O₂ at 30-35°C using as catalyst a sample of Ru(bpy)₃-APTES@PDA@PUF of *ca.* 1.5 cm × 1.5 cm × 3 cm, whose mass was adjusted in relation to its Ru content established by ICP-AES to reach a Ru loading of 0.9 mol% (Table S1). Solvents and lights were found to have a prominent influence on the conversion. In acetonitrile under blue light (LED, 18W), the reaction conversion reached 59 % after 24 h and 90 % after 48 h, with complete selectivity to *N*-benzylbenzaldimine. Solvents such as methanol, toluene and acetonitrile/water all proved less

suitable for the reaction under otherwise similar conditions, giving much lower conversions after 24 h reaction. The use of white light (LED, 24 W) also resulted in a lower conversion after 24 h (47% conversion vs. 59% under 18W blue LED light after 24 h reaction). Not surprisingly [74], the reactive rate of the supported catalyst was much slower than that of its homogeneous counterpart, $[\text{Ru}(\text{bpy})_3\text{Cl}_2] \cdot 6\text{H}_2\text{O}$, which achieved 84% conversion in 1 h under similar conditions. Nevertheless, the benefit in using the foam lies in that the latter could be reused multiple times, tolerating repeated solvents rinsing and immersions without apparent deactivation, as a single sample of $\text{Ru}(\text{bpy})_3\text{-APTES@PDA@PUF}$ was used for these optimization studies. Furthermore, as expected, the absence of structured catalyst or light led to the absence of reaction, thus demonstrating that supported Ru photocatalysis was at the origin of the reaction [75]. Finally, the use of a cubic sample of PDA@PUF also resulted in the absence of reaction, showing that the support by itself is not able to induce the catalytic process.

With these optimized conditions in hands (CH_3CN , 18W blue LED light, 48 h), the scope of the homocouplings was then briefly evaluated with a single sample of $\text{Ru}(\text{bpy})_3\text{-APTES@PDA@PUF}$ ($1.5 \text{ cm} \times 1.5 \text{ cm} \times 3 \text{ cm}$, 0.9 mol% Ru) (Fig. 5). *para*-Substituted benzylamines bearing electron-donating methoxy or *t*-butyl substituents were converted in high yields (89 % and 95 %) within 48 h reaction time, similarly to benzylamine. In contrast, when benzylamine was *para*-substituted with electron-withdrawing substituents such as trifluoromethyl and chloride, slightly lower conversions of 77 % and 82 % conversion were observed after 48 h reaction, in agreement with the literature, as electron-poor benzylamines typically give lower yields in this type of oxidative couplings [50-58]. Additionally, the photocatalytic activity of $\text{Ru}(\text{bpy})_3\text{-APTES@PDA@PUF}$ was explored for the oxidative homocoupling of the heterocyclic amine, 2-pyridinemethanamine, resulting in 77% conversion after 48 h. Noteworthy, the catalytic foam seemed stable and robust all along the

scope study, as suggested by these results.

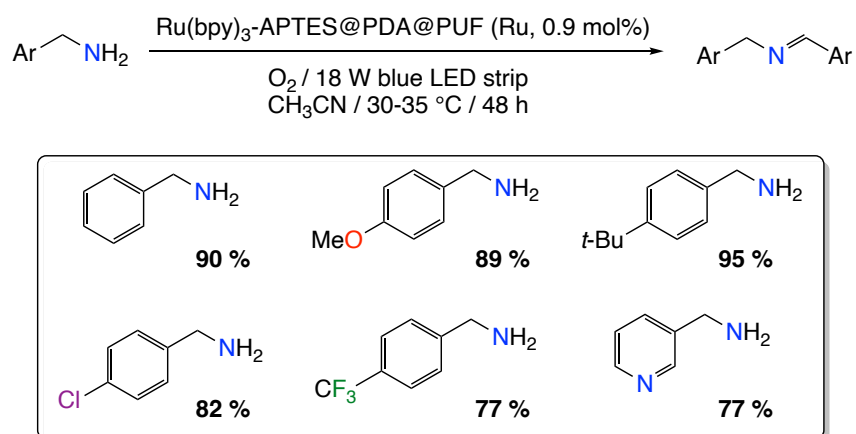


Figure 5. Oxidative homocoupling of benzylic amines using Ru(bpy)₃-APTES@PDA@PUF as photocatalyst.

In order to further probe and evaluate the photocatalytic performances of Ru(bpy)₃-APTES@PDA@PUF, oxidative C–H bond functionalizations of *N*-phenyl-tetrahydroisoquinoline were selected as a second type of model reactions given the universality of this elegant reaction for [Ru(bpy)₃]Cl₂-mediated photocatalysis [36,50,59-63]. Using a sample of Ru(bpy)₃-APTES@PDA@PUF of *ca.* 1.5 cm × 1.5 cm × 3 cm, whose mass was adjusted to have a Ru loading of 4.5 mol%, as photocatalyst, O₂ as oxidant, under an 18W blue LED light [76], we first focused on the reaction between *N*-phenyl-tetrahydroisoquinoline and nitromethane in order to optimize the reactions conditions (Table S2). As observed for the oxidative homocoupling of benzylic amines, solvents were found to have a significant influence on the progress of the reaction, and, in agreement with the literature [36], methanol was found to be the one giving the best results. Thus, in methanol at *ca.* 30-35 °C, the reaction yield could reach up to 83 % after 24 h reaction when a large excess of nitromethane (20 equiv.) was used.

With these conditions in hands (NuH (20 equiv.), MeOH, 18W blue LED light, 24 h), the scope of this cross dehydrogenative coupling was then evaluated with a short series of

nucleophiles, using a single sample of Ru(bpy)₃-APTES@PDA@PUF (1.5 cm × 1.5 cm × 3 cm, 4.5 mol% Ru). All investigated nucleophiles, including secondary phosphine oxides, gave the desired reaction compounds in yields varying from 23 to 62 % (Fig. 6). Satisfyingly again, the heterogeneous photocatalyst proved stable throughout the reaction scope investigation, as it could be used for one substrate after another without any apparent deactivation or inhibition.

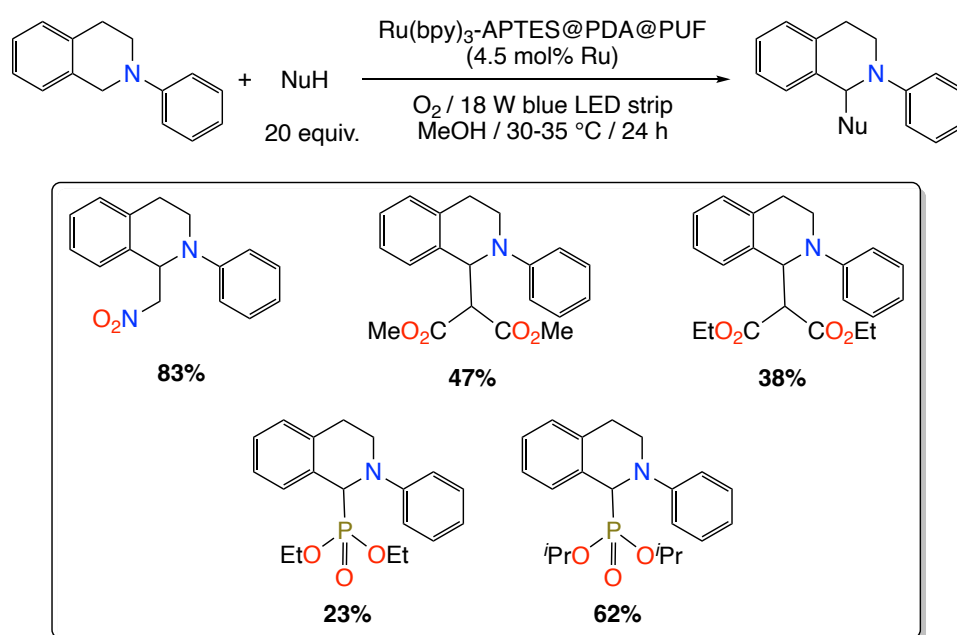


Figure 6. Photocatalytic C–C / C–P couplings N-phenyl-tetrahydroisoquinoline with various nucleophiles using Ru(bpy)₃-APTES@PDA@PUF as photocatalyst.

3.3. Catalyst recycling and leaching tests

For heterogeneous catalytic systems, the catalyst recovery from liquid media and its reuse are of great significance. With powdered catalysts, tedious and time-consuming work-up procedures, as well as problems of catalyst loss are usually inevitable. The macroscopically structured catalyst used in the present work allows one to operate the product-catalyst separation in a much easier way as the catalyst can be just taken out from the reaction medium and quickly washed to remove the adsorbed liquid on its surface before

being reused.

To shed more light on the recycling properties of Ru(bpy)₃-APTES@PDA@PUF that could be foreseen from the optimization and scope studies (*vide supra*), six consecutive runs of benzylamine oxidative homocoupling and of *N*-phenyl-tetrahydroisoquinoline nitromethylation were conducted; each with a single sample of freshly prepared Ru(bpy)₃-APTES@PDA@PUF (1.5 cm × 1.5 cm × 3 cm, 4.5 μmol Ru) that was simply removed from the reaction medium and washed in various solvents under sonication after each run, before being reused. Strikingly, the photocatalytic activity stayed at an excellent level for the 6 runs in both reactions, with a notable improvement of the observed GC conversions or NMR yields from run 1 to 3 in the oxidative benzylamine coupling (Fig. 7A) and from run 1 to 6 in the nitromethylation of *N*-phenyl-tetrahydroisoquinoline (Fig. 7B). The reason for this gradual improvement of the photocatalytic activity of Ru(bpy)₃-APTES@PDA@PUF was not clear but we suspected it could be related to a modification of the uppermost layer of the PDA coating as suggested by the colour lightening of the foam from dark brown to brown-red or even orange, depending on the considered reaction (Fig. S8).

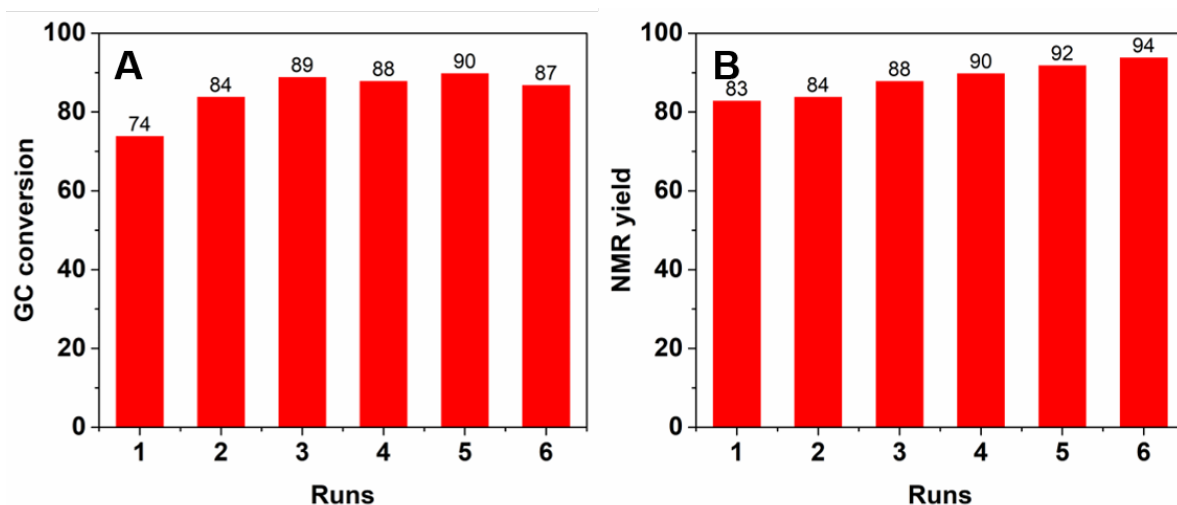


Figure 7. GC conversions and NMR yields measured over the 6 successive runs of oxidative homocoupling of benzylamine (A) and of nitromethylation of *N*-phenyl-tetrahydroisoquinoline (B) catalysed by a single sample of Ru(bpy)₃-APTES@PDA@PUF in each case. Benzylamine homocoupling conditions: benzylamine (0.5 mmol), Ru(bpy)₃-APTES@PDA@PUF (1.5 cm × 1.5 cm × 3 cm, 4.5 μmol Ru, *i.e.*: 0.9 mol%), CH₃CN (10 mL), O₂ balloon, 18 W blue LED light, 30-35 °C, 48 h, 1000 rpm, GC conversions uncertainties: ± 1%. Aza-Henry conditions: 2-phenyl-1,2,3,4-tetrahydroisoquinoline (0.1 mmol), nitromethane (2 mmol), Ru(bpy)₃-APTES@PDA@PUF (1.5 cm × 1.5 cm × 3 cm, 4.5 μmol Ru, *i.e.*: 4.5 mol%), MeOH (10 mL), O₂ balloon, 18 W blue LED light, 30-35 °C, 24 h, 1000 rpm, NMR yields uncertainties: ± 1%.

To try to gain some insight about this apparent modification of the foam surface, the spent foam after 6 cycles of oxidative benzylamine coupling was submitted to SEM and SEM-EDX analyses. Low magnification SEM images showed a higher degree of corrugation of the struts' edges (Fig. 8), due most probably to repeated solvent swelling in the polymeric foam [12]. In contrast, higher magnification images revealed a smoother surface with less numerous scattered PDA aggregates (Fig. 8), which may be at the origin of the observed colour lightening as well as of a better access of the substrates to the immobilised Ru catalyst which, in return, could explain the progressive increase of activity observed over the cycling

tests. Noteworthy, the elemental distribution over the foam surface did not seem to be significantly affected by this surface smoothing as SEM-EDX elemental mapping still showed a relatively homogeneous distribution of C, N, O, Si and Ru elements over the foam surface without apparent aggregates or segregations area (Fig. S9 and S10). In agreement with these results, the XPS survey scan and high-resolution spectra still showed the core levels of O1s, N1s, C1s, Si2p and Ru3d elements (Fig. S6B, S7). When compared to that of the as-synthesized foam, the high-resolution spectra of the C1s, Ru3d_{5/2} and Si2p core level regions however revealed that the relative level of Ru3d_{5/2} (when compared to that of C1s) has decreased, which suggests some Ru leaching, while that of Si2p had comparatively increased (at least on the topmost surface), which may explain the better accessibility of the remaining Ru photocatalyst (Fig. S7). This was partly confirmed by ICP-AES analyses of the spent Ru(bpy)₃-APTES@PDA@PUF catalytic material, which indicated a loss of Ru of about 30% (1.404 ± 0.016 g/kg vs. 2.024 ± 0.027 g/kg for the as synthesized foam) while the amount of Si level did not vary significantly (1.564 ± 0.020 to 1.633 ± 0.018 g/kg). Noteworthy this Ru loss was also confirmed by ICP-AES analyses of the reaction solutions, which indicated a similar loss of about 30% over the 6 cycles, but with decreasing amounts at each run, *i.e.*: from 3.77 ± 0.02 mg/kg in the first run to 1.56 mg/kg ± 0.01 in the last one. All this suggests that the catechol-silicon linkage, whether linear or cross-linked, was stable enough to sustain the reaction conditions along the six cycling runs, in agreement with our previous results on supported molecular catalysts bearing an alkoxysilyl anchoring arm on PDA@PUF foams [12]. Furthermore, the fact that, despite this stability of the catechol-silicon linkage, some Ru leaching was observed, suggest however that either some Ru(bpy)₂Cl₂ was simply adsorbed on the PDA layer or more likely that the amide linkage between the siloxytriethylamino anchor and the bipyridine was not stable under the reaction conditions.

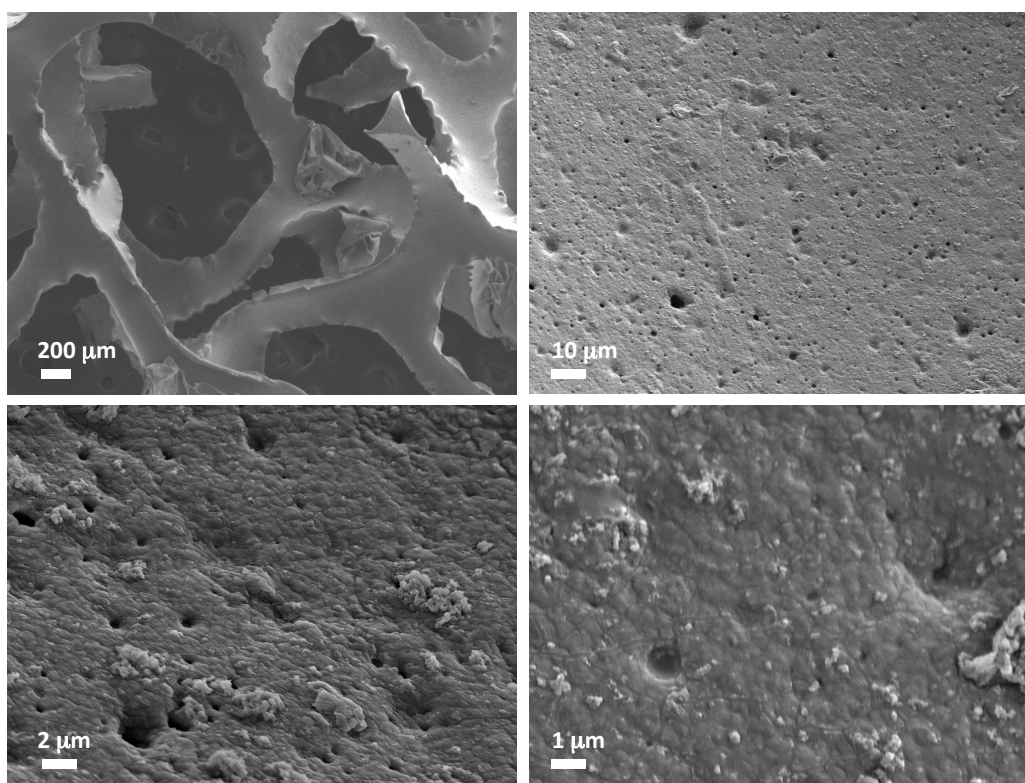


Figure 8. SEM images with different magnifications of spent $\text{Ru}(\text{bpy})_3\text{-APTES@PDA@PUF}$ after six cycles of oxidative homocoupling of benzylamine.

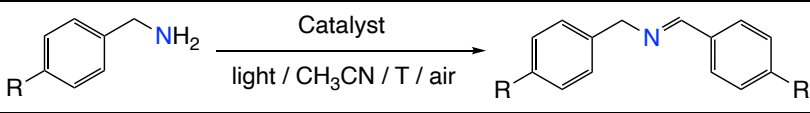
Finally, to evaluate the influence of the Ru leaching in the liquid reaction medium on the progress of a photocatalytic process with an as-synthesized sample of $\text{Ru}(\text{bpy})_3\text{-APTES@PDA@PUF}$, a control experiment was carried out where, after 8 h reaction, the reaction solution of a *N*-phenyl-tetrahydroisoquinoline nitromethanation was diluted twice and split into two equal portions; one of which was allowed to continue the reaction in the presence of the catalytic foam while the other was maintained under similar conditions but without the catalytic foam. While the NMR yield was of 7% after the first 8 h reaction, it reached 60 % after 24 h in the case of the foam-catalysed reaction and 21% in the case of the blank reaction (Fig. S11). This shows that, at least for the first run with an as-synthesized foam, the leached Ru has a non-negligible influence on the reaction course but that most of the activity is nevertheless due to the heterogeneous catalyst.

3.4. Comparison with other Ru(bpy)₃²⁺-based heterogeneous catalysts

Interestingly, Ru(bpy)₃-APTES@PDA@PUF compares well with the very rare examples from the literature, where Ru(bpy)₃²⁺ has been incorporated in various supports for the oxidative coupling of benzylamines under visible-light irradiation and aerobic conditions [50-52]. Independently on the type of support – almost non-porous (Ru-1 and Ru-2 [52]) and non-porous (Ru-CP [51]) cross-linked polymers or in UiO-67 metal-organic framework (MOF-6 [50]) – these heterogeneous Ru(bpy)₃²⁺-based catalysts indeed all required much harder reaction conditions (300 or 450 W Xe lamps at 60 °C vs. 18 W blue led at 30-35 °C) to give similar TON values (Table 1, entries 3-10 vs. 1-2). Furthermore, if some of them could be reused a couple of time (entries 4-5, 7-8 and 9-10) without significant loss of activity, none was reused 6 times like Ru(bpy)₃-APTES@PDA@PUF.

Regarding the aza-Henry reaction, if one consider the observed TON and TOF values, Ru(bpy)₃-APTES@PDA@PUF compares less favorably with the rare examples from the literature, where Ru(bpy)₃²⁺ has been used under homogeneous conditions [59], incorporated in porous (Ru-PCP [60]), almost non-porous (Ru-1 and Ru-2 [52]) and non-porous Ru-CP [51]) cross-linked polymers, in mesoporous organic polymer (Ru-POP) [61], or in UiO-67 metal-organic frameworks (MOF-6 [50]). The TON and TOF values observed with Ru(bpy)₃-APTES@PDA@PUF are indeed 4 to 23 and 4 to 135 times lower, respectively, than those observed with these other Ru(bpy)₃²⁺-based photocatalysts (Table 2, entries 1-2 vs. entries 3-13). Nevertheless, if one considers the reusing abilities of the various heterogeneous catalysts, Ru(bpy)₃-APTES@PDA@PUF shows superior abilities to the latter. It can indeed be used up to 6 times with a steady increase of its activity (as described in section 3.3), whereas Ru-1, MOF-6 and to a lesser extent Ru-CP all show a significant decrease of activity in only 3 to 5 runs (Table 2, entries 6-7, 9-10 and 12-13).

Table 1. Oxidative coupling of benzylamines under visible light irradiation and aerobic conditions using Ru(bpy)₃²⁺ heterogenized on various supports as photocatalyst.

							
Entry	Catalyst (mol%)	Light	Temp. (°C)	Time (h)	GC or NMR yield (%)	TON ^a	TOF (h ⁻¹) ^b
1 ^{c,d}	Ru(bpy) ₃ -APTES@PDA@PUF (0.9)	18 W blue LED	30-35	48	74	41.1	0.86
2 ^{c,d}	Ru(bpy) ₃ -APTES@PDA@PUF (0.9) 6th run	18 W blue LED	30-35	48	87	48.3	1.0
3 ^{c,f}	Ru-1 (1)	450 W Xe lamp	60	1	93	46.5	46.5
4 ^{e,f}	Ru-1 (1)	450 W Xe lamp	60	1	88	44	44
5 ^{e,f}	Ru-1 (1) 3rd run	450 W Xe lamp	60	1	84	42	42
6 ^{c,f}	Ru-2 (1)	450 W Xe lamp	60	1	88	44	44
7 ^{c,g}	Ru-CP (1)	450 W Xe lamp	60	1	99	49.5	49.5
8 ^{c,g}	Ru-CP (1) 3rd run	450 W Xe lamp	60	1	99	49.5	49.5
9 ^{c,h}	MOF-6 (1)	300 W Xe lamp	60	1	83	41.5	41.5
10 ^{c,h}	MOF-6 (1) 2nd run	300 W Xe lamp	60	1	80	40	40

^a TON expressed as the (conversion / catalyst loading) / 2. ^b TOF (h⁻¹) expressed as the TON / reaction time (h). ^c R = H. ^d This work. ^e R = Me. ^f Results from ref. [52]. ^g Results from ref. [51]. ^h Results from ref. [50].

Table 2. Nitromethylation of *N*-phenyl-tetrahydroisoquinoline under visible light irradiation and aerobic conditions using Ru(bpy)₃²⁺ heterogenized on various supports as photocatalyst.

Entry	Catalyst (mol%)	Solvent	Light	Temp. (°C)	Time (h)	NMR yield (%)	Isolated yield (%)	TON ^a	TOF (h ⁻¹) ^b
1 ^{c,d}	Ru(bpy) ₃ -APTES@PDA@PUF (4.5)	CH ₃ OH	18 W blue LED	30-35	24	-	83	18	0.8
2 ^{c,d}	Ru(bpy) ₃ -APTES@PDA@PUF (4.5) 6th run	CH ₃ OH	18 W blue LED	30-35	24	94	-	21	0.9
3 ^{c,e}	Ru(bpy) ₃ Cl ₂ (1)	CH ₃ NO ₂	26 W fluorescent lamp	RT	20	100	81	81	4.1
4 ^{c,f}	Ru-PCP (0.2)	CH ₃ NO ₂	26 W fluorescent lamp	RT	8	90	-	450	56.3
5 ^{c,g}	Ru-1 (0.2)	CH ₃ NO ₂	26 W fluorescent lamp	RT	8	94	85	425	53.1
6 ^{g,h}	Ru-1 (0.2)	CH ₃ NO ₂	26 W fluorescent lamp	RT	8	99	89	445	55.6
7 ^{g,h}	Ru-1 (0.2) 4th run	CH ₃ NO ₂	26 W fluorescent lamp	RT	8	87	76	380	47.5
8 ^{c,g}	Ru-2 (0.2)	CH ₃ NO ₂	26 W fluorescent lamp	RT	8	92	81	405	50.6
9 ^{c,i}	Ru-CP (0.2)	CH ₃ NO ₂	26 W fluorescent lamp	RT	8	97	-	485	60.6
10 ^{c,i}	Ru-CP (0.2) 5th run	CH ₃ NO ₂	26 W fluorescent lamp	RT	8	92	-	460	57.5
11 ^{c,j}	Ru-POP (0.2)	CH ₃ NO ₂	24 W bulb	RT	4	-	97	485	121.3
12 ^{c,k}	MOF-6 (1)	CH ₃ NO ₂	26 W fluorescent lamp	RT	12	86	-	86	7.2
13 ^{c,k}	MOF-6 (1) 3rd run	CH ₃ NO ₂	26 W fluorescent lamp	RT	12	62	-	62	5.2

^a TON expressed as the isolated (or NMR) yield / catalyst loading. ^b TOF (h⁻¹) expressed as the TON / reaction time (h). ^c R = H. ^d This work. ^e Results from ref. [59]. ^f Results from ref. [60]. ^g Results from ref. [52]. ^h R = Br. ⁱ Results from ref. [51]. ^j Results from ref. [61]. ^k Results from ref. [50].

4. Conclusion

In summary, we have prepared a macroscopic Ru(bpy)₃-functionalized open cell polymeric foam that functioned as a versatile heterogeneous photocatalyst. Following a simple dip-coating protocol of an open cell polyurethane foam in an aqueous solution of

dopamine, the resulting polydopamine-coated foam, PDA@PUF, was functionalized with $\text{Ru}(\text{bpy})_3^{2+}$ via a three-step route involving a silanization process of the mussel-inspired adhesive layer with APTES, the subsequent EDC-mediated coupling with [2,2'-bipyridine]-4-carboxylic acid and the complexation of the anchored bipyridine with $[\text{Ru}(\text{bpy})_2\text{Cl}_2]$.

The resulting $\text{Ru}(\text{bpy})_3\text{-APTES@PDA@PUF}$ material acted as an efficient heterogeneous photocatalyst for both oxidative benzylic amine homocouplings and cross dehydrogenative couplings under visible-light irradiation and molecular oxygen as a green oxygen source, and showed excellent reusability for at least 6 runs in an easy-to-carry “dip-and-play” mode allowed by its macroscopic structure. Despite the fact that about 30% ruthenium leaching was observed over the 6 cycling tests – which most probably results from the sensitivity of the amide linkage but not from that of the alkoxysilyl anchor, as demonstrated by ICP-AES analyses – an improvement of the catalytic performances was observed over the successive cycling tests in both reactions. As suggested by a combination of photographs, SEM and XPS analyses, this unexpected improvement most likely results from a modification of the uppermost layer of polydopamine that renders the $[\text{Ru}(\text{bpy})_3]^{2+}$ photocatalyst more accessible.

Provided that more solid chemical links than the amide linkage will be used in the future, these results pave the way for the design of easy-to-handle long-lived heterogeneous photocatalysts whose easy-to engineer flexible macroscopic structure with large pores allowing efficient mass transfers, low pressure drop, and easy light penetration should permit their use under flow conditions in industrial photoreactors.

Declaration of Competing Interest

The authors declare that they have no known competing financial interests or personal relationships that could have appeared to influence the work reported in this paper.

Acknowledgements

This work supported by the University of Strasbourg (IdEx Unistra 2019). H.P. thanks the International Doctoral Program of the Université de Strasbourg for his PhD fellowship. The authors thank the NMR and Analytical Platform managers of LIMA, Dr Emeric Wasielewski and Mr. Matthieu Chesse, who contributed, by their valuable technical support, to the completion of this research project.

Appendix. Supplementary materials

Supplementary materials to this article can be found online at <https://doi.org/10.1016/j.mcat.2023.xxxx>.

References and Notes

-
- [1] J.J.W. Bakker, W.J. Groendijk, K.M. de Lathouder, F. Kapteijn, J.A. Moulijn, M.T. Kreutzer, S.A. Wallin, Enhancement of catalyst performance using pressure pulses on macroporous structured catalysts, *Ind. Eng. Chem. Res.* 46 (2007) 8574-8583, <http://doi.org/10.1021/ie070033o>.
 - [2] L. Giani, G. Groppi, E. Tronconi, Mass-transfer characterization of metallic foams as supports for structured catalysts, *Ind. Eng. Chem. Res.* 44 (2005) 4993-5002, <http://doi.org/10.1021/ie0490886>.
 - [3] J.T. Richardson, Y. Peng, D. Remue, Properties of ceramic foam catalyst supports: pressure drop, *Appl. Catal. A* 204 (2000) 19-32, [http://doi.org/10.1016/S0926-860X\(00\)00508-1](http://doi.org/10.1016/S0926-860X(00)00508-1).
 - [4] M. Lacroix, P. Nguyen, D. Schweich, C.P. Huu, S. Savin-Poncet, D. Edouard, Pressure drop measurements and modeling on SiC foams, *Chem. Eng. Sci.* 62 (2007) 3259-3267, <http://doi.org/10.1016/j.ces.2007.03.027>.
 - [5] M. Lacroix, L. Dreibine, B. de Tymowski, F. Vigneron, D. Edouard, D. Bégin, P. Nguyen, C. Pham, S. Savin-Poncet, F. Luck, M.-J. Ledoux, C. Pham-Huu, Silicon carbide foam composite containing cobalt as a highly selective and re-usable Fischer-

-
- Tropsch synthesis catalyst, *Appl. Catal. A* 397 (2011) 62-72, <http://doi.org/10.1016/j.apcata.2011.02.012>.
- [6] H.W. Engels, H.G. Pirkel, R. Albers, R.W. Albach, J. Krause, A. Hoffmann, H. Casselmann, J. Dormish, Polyurethanes: versatile materials and sustainable problem solvers for today's challenges, *Angew. Chem. Int. Ed.* 52 (2013) 9422-9441, <http://doi.org/10.1002/anie.201302766>.
- [7] H. Lee, S.M. Dellatore, W.M. Miller, P.B. Messersmith, Mussel-inspired surface chemistry for multifunctional coatings, *Science* 318 (2007) 426-430, <http://doi.org/10.1126/science.1147241>.
- [8] D. Edouard, V. Ritleng, L. Jierry, N.T.T. Chau, Method for modifying the surface properties of elastomer cellular foams, WO 2016012689A2, 2016.
- [9] E. Pardieu, N.T.T. Chau, T. Dintzer, T. Romero, D. Favier, T. Roland, D. Edouard, L. Jierry, V. Ritleng, Polydopamine-coated open cell polyurethane foams as an inexpensive, flexible yet robust catalyst support: a proof of concept, *Chem. Commun.* 52 (2016) 4691-4693, <http://doi.org/10.1039/c6cc00847j>.
- [10] L. Lefebvre, J. Kelber, L. Jierry, V. Ritleng, D. Edouard, Polydopamine-coated open cell polyurethane foam as an efficient and easy-to-regenerate soft structured catalytic support (S₂CS) for the reduction of dye, *J. Environ. Chem. Eng.* 5 (2017) 79-85, <http://doi.org/10.1016/j.jece.2016.11.025>.
- [11] L. Lefebvre, J. Kelber, X. Mao, F. Ponzio, G. Agusti, C. Vigier-Carrière, V. Ball, L. Jierry, V. Ritleng, D. Edouard, Borohydride-functionalized polydopamine-coated open cell polyurethane foam as a reusable soft structured material for reduction reactions: application to the removal of a dye, *Environ. Prog. Sustain. Energy* 38 (2019) 329-335, <http://doi.org/10.1002/ep.12944>.
- [12] A. Ait Khouya, M.L. Mendez Martinez, P. Bertani, T. Romero, D. Favier, T. Roland, V. Guidal, V. Bellière-Baca, D. Edouard, L. Jierry, V. Ritleng, Coating of polydopamine on polyurethane open cell foams to design soft structured supports for molecular catalysts, *Chem. Commun.* 55 (2019) 11960-11963, <http://doi.org/10.1039/C9CC05379D>.
- [13] L. Birba, V. Ritleng, L. Jierry, G. Agusti, P. Fongarland, D. Edouard, An efficient bio-inspired catalytic tool for hydrogen release at room temperature from a stable borohydride solution, *Int. J. Energy Res.* 44 (2020) 10612-10627, <http://doi.org/10.1002/er.5702>.

-
- [14] F. Ponzio, J. Kelber, L. Birba, K. Reka, V. Ritleng, L. Jarry, D. Edouard, Polydopamine film coating on polyurethane foams as efficient “sunscreen”. Application to photocatalysis under UV irradiation, *Environ. Technol. Innov.* 23 (2021) 101618, <http://doi.org/10.1016/j.eti.2021.101618>.
- [15] H. Peng, X. Zhang, V. Papaefthimiou, C. Pham-Huu, V. Ritleng, Pd-functionalized polydopamine-coated polyurethane foam: a readily prepared and highly reusable structured catalyst for selective alkyne semi-hydrogenation and Suzuki coupling under air, *Green Chem.* 25 (2023) 264–279, <https://doi.org/10.1039/D2GC03283J>.
- [16] H. Peng, T. Romero, P. Bertani, V. Ritleng, Polydopamine-coated polyurethane foam as a structured support for the development of an easily reusable heterogeneous photocatalyst based on Eosin Y, *Catalysts* 13 (2023) 589, <https://doi.org/10.3390/catal13030589>.
- [17] J. Saiz-Poseu, J. Mancebo-Aracil, F. Nador, F. Busqué, D. Ruiz-Molina, The chemistry behind catechol-based adhesion, *Angew. Chem. Int. Ed.* 58 (2019) 696–714, <https://doi.org/10.1002/anie.201801063>.
- [18] D.M. Arias-Rotondo, J.K. McCusker, The photophysics of photoredox catalysis: a roadmap for catalyst design, *Chem. Soc. Rev.* 45 (2016) 5803–5820, <https://doi.org/10.1039/C6CS00526H>.
- [19] C.K. Prier, D.A. Rankic, D.W. MacMillan, Visible light photoredox catalysis with transition metal complexes: applications in organic synthesis, *Chem. Rev.* 113 (2013) 5322–5363, <https://doi.org/10.1021/cr300503r>.
- [20] J.M. Narayanam, J.W. Tucker, C.R. Stephenson, Electron-transfer photoredox catalysis: development of a tin-free reductive dehalogenation reaction, *J. Am. Chem. Soc.* 131 (2009) 8756–8757, <https://doi.org/10.1021/ja9033582>.
- [21] J.W. Beatty, C.R. Stephenson, Amine functionalization via oxidative photoredox catalysis: methodology development and complex molecule synthesis, *Acc. Chem. Res.* 48 (2015) 1474–1484, <https://doi.org/10.1021/acs.accounts.5b00068>.
- [22] Y.Q. Zou, J.R. Chen, X.P. Liu, L.Q. Lu, R.L. Davis, K.A. Jørgensen, W.J. Xiao, Highly efficient aerobic oxidative hydroxylation of arylboronic acids: photoredox catalysis using visible light, *Angew. Chem. Int. Ed.* 51 (2012) 784–788, <https://doi.org/10.1002/anie.201107028>.

-
- [23] M.A. Ischay, M.E. Anzovino, J. Du, T.P. Yoon, Efficient visible light photocatalysis of [2+2] enone cycloadditions, *J. Am. Chem. Soc.* 130 (2008) 12886-12887, <https://doi.org/10.1021/ja805387f>.
- [24] T.P. Yoon, M.A. Ischay, J. Du, Visible light photocatalysis as a greener approach to photochemical synthesis, *Nat. Chem.* 2 (2010) 527-532, <https://doi.org/10.1038/nchem.687>.
- [25] P. Pali, G. Shukla, P. Saha, M.S. Singh, Photo-oxidative Ruthenium(II)-Catalyzed Formal [3+2] Heterocyclization of Thioamides to Thiadiazoles, *Org. Lett.* 23 (2021) 3809-3813, <https://doi.org/10.1021/acs.orglett.1c00766>.
- [26] T.P. Yoon, Visible light photocatalysis: the development of photocatalytic radical ion cycloadditions, *ACS Catal.* 3 (2013) 895-902, <https://doi.org/10.1021/cs400088e>.
- [27] L.-M. Zhao, T. Lei, R.-Z. Liao, H. Xiao, B. Chen, V. Ramamurthy, C.-H. Tung, L.-Z. Wu, Visible-Light-Triggered Selective Intermolecular [2+2] Cycloaddition of Extended Enones: 2-Oxo-3-enoates and 2,4-Dien-1-ones with Olefins, *J. Org. Chem.* 84 (2019) 9257-9269, <https://doi.org/10.1021/acs.joc.9b01273>.
- [28] K. Zhang, L. Qiao, J. Xie, Z. Lin, H. Li, P. Lu, Y. Wang, Visible-Light-Induced C(sp²)-C(sp³) Coupling Reaction for the Regioselective Synthesis of 3-Functionalized Coumarins, *J. Org. Chem.* 86 (2021) 9552-9562, <https://doi.org/10.1021/acs.joc.1c00848>.
- [29] H.-Y. Zhang, J. Chen, C.-C. Lu, Y.-P. Han, Y. Zhang, J. Zhao, Visible-Light-Induced C(sp²)-C(sp³) Cross-Dehydrogenative-Coupling Reaction of N-Heterocycles with N-Alkyl-N-methylanilines under Mild Conditions, *J. Org. Chem.* 86 (2021) 11723-11735, <https://doi.org/10.1021/acs.joc.1c01207>.
- [30] M. Jouffroy, D.N. Primer, G.A. Molander, Base-Free Photoredox/Nickel Dual-Catalytic Cross-Coupling of Ammonium Alkylsilicates, *J. Am. Chem. Soc.* 138 (2016) 475-478, <https://doi.org/10.1021/jacs.5b10963>.
- [31] J. Xu, K. Jung, C. Boyer, Oxygen tolerance study of photoinduced electron transfer-reversible addition-fragmentation chain transfer (PET-RAFT) polymerization mediated by Ru(bpy)₃Cl₂, *Macromolecules* 47 (2014) 4217-4229, <https://doi.org/10.1021/ma500883y>.
- [32] J. Yeow, J. Xu, C. Boyer, Polymerization-Induced Self-Assembly Using Visible Light Mediated Photoinduced Electron Transfer-Reversible Addition-Fragmentation Chain

-
- Transfer Polymerization, ACS Macro Lett. 4 (2015) 984-990, <https://doi.org/10.1021/acsmacrolett.5b00523>.
- [33] D.A. Nicewicz, D.W. MacMillan, Merging photoredox catalysis with organocatalysis: the direct asymmetric alkylation of aldehydes, Science 322 (2008) 77-80, <https://doi.org/10.1126/science.1161976>.
- [34] M. Li, Y. Sang, X.-S. Xue, J.-P. Cheng, Origin of Stereocontrol in Photoredox Organocatalysis of Asymmetric α -Functionalizations of Aldehydes, J. Org. Chem. 83 (2018) 3333-3338, <https://doi.org/10.1021/acs.joc.8b00469>.
- [35] J.J. Douglas, M.J. Sevrin, C.R.J. Stephenson, Visible Light Photocatalysis: Applications and New Disconnections in the Synthesis of Pharmaceutical Agents, Org. Process Res. Dev. 20 (2016) 1134-1147, <https://doi.org/10.1021/acs.oprd.6b00125>.
- [36] A.A. Yakushev, A.S. Abel, A.D. Averin, I.P. Beletskaya, A.V. Cheprakov, I.S. Ziankou, L. Bonneviot, A. Bessmertnykh-Lemeune, Visible-light photocatalysis promoted by solid- and liquid-phase immobilized transition metal complexes in organic synthesis, Coord. Chem. Rev. 458 (2022) 214331, <https://doi.org/10.1016/j.ccr.2021.214331>.
- [37] H.-W. Hsieh, C.W. Coley, L.M. Baumgartner, K.F. Jensen, R.I. Robinson, Photoredox Iridium–Nickel Dual-Catalyzed Decarboxylative Arylation Cross-Coupling: From Batch to Continuous Flow via Self-Optimizing Segmented Flow Reactor, Org. Process Res. Dev. 22 (2018) 542-550, <https://doi.org/10.1021/acs.oprd.8b00018>.
- [38] K. Mori, D. Tatsumi, T. Iwamoto, Y. Masui, M. Onaka, H. Yamashita, Ruthenium(II)–Bipyridine/Nano C₃N₄ Hybrids: Tunable Photochemical Properties by Using Exchangeable Alkali Metal Cations, Chem. Asian J. 13 (2018) 1348-1356, <https://doi.org/10.1002/asia.201800397>.
- [39] X. Li, Z. Hao, F. Zhang, H. Li, Reduced graphene oxide-immobilized tris(bipyridine)ruthenium(II) complex for efficient visible-light-driven reductive dehalogenation reaction, ACS Appl. Mater. Interfaces 8 (2016) 12141-12148, <https://doi.org/10.1021/acsami.6b01100>.
- [40] J. Pang, S. Yuan, J.-S. Qin, C. T. Lollar, N. Huang, J. Li, Q. Wang, M. Wu, D. Yuan, M. Hong, H.-C. Zhou, Tuning the ionicity of stable metal–organic frameworks through ionic linker installation, J. Am. Chem. Soc. 141 (2019) 3129-3136, <https://doi.org/10.1021/jacs.8b12530>.

-
- [41] Y.-P. Wu, B. Yang, J. Tian, S.-B. Yu, H. Wang, D.-W. Zhang, Y. Liu, Z.-T. Li, Postmodification of a supramolecular organic framework: visible-light-induced recyclable heterogeneous photocatalysis for the reduction of azides to amines, *Chem. Commun.* 53 (2017) 13367-13370, <https://doi.org/10.1039/C7CC08824H>.
- [42] A. Xie, K. Zhang, F. Wu, N. Wang, Y. Wang, M. Wang, Polydopamine nanofilms as visible light-harvesting interfaces for palladium nanocrystal catalyzed coupling reactions, *Catal. Sci. Technol.* 6 (2016) 1764-1771, <https://doi.org/10.1039/C5CY01330E>.
- [43] M. Lee, J. U. Kim, J. S. Lee, B. I. Lee, J. Shin, C.B. Park, Nanostructures: Mussel-Inspired Plasmonic Nanohybrids for Light Harvesting, *Adv. Mater.* 26 (2014) 4463-4468, <https://doi.org/10.1002/adma.201305766>.
- [44] J.H. Kim, M. Lee, C.B. Park, Polydopamine as a Biomimetic Electron Gate for Artificial Photosynthesis, *Angew. Chem. Int. Ed.* 53 (2014) 6364-6368, <https://doi.org/10.1002/anie.201402608>.
- [45] P. Xia, M. Liu, B. Cheng, J. Yu, L. Zhang, Dopamine Modified g-C₃N₄ and Its Enhanced Visible-Light Photocatalytic H₂-Production Activity, *ACS Sustain. Chem. Eng.* 6 (2018) 8945-8953, <https://doi.org/10.1021/acssuschemeng.8b01300>.
- [46] Z. Yu, F. Li, Q. Yang, H. Shi, Q. Chen, M. Xu, Nature-Mimic Method To Fabricate Polydopamine/Graphitic Carbon Nitride for Enhancing Photocatalytic Degradation Performance, *ACS Sustain. Chem. Eng.* 5 (2017) 7840-7850, <https://doi.org/10.1021/acssuschemeng.7b01313>.
- [47] H. Wang, Q. Lin, L. Yin, Y. Yang, Y. Qiu, C. Lu, H. Yang, Biomimetic Design of Hollow Flower-Like g-C₃N₄@PDA Organic Framework Nanospheres for Realizing an Efficient Photoreactivity, *Small* 15 (2019) 1900011, <https://doi.org/10.1002/sml.201900011>.
- [48] C. Zhang, H.-C. Yang, L.-S. Wan, H.-Q. Liang, H. Li, Z.-K. Xu, Polydopamine-Coated Porous Substrates as a Platform for Mineralized β -FeOOH Nanorods with Photocatalysis under Sunlight, *ACS Appl. Mater. Interfaces* 7 (2015) 11567-11574, <https://doi.org/10.1021/acsami.5b02530>.
- [49] W.-X. Mao, X.-J. Lin, W. Zhang, Z.-X. Chi, R.-W. Lyu, A.-M. Cao, L.-J. Wan, Core-shell structured TiO₂@polydopamine for highly active visible-light photocatalysis, *Chem. Commun.* 52 (2016) 7122-7125, <https://doi.org/10.1039/C6CC02041K>.

-
- [50] C. Wang, Z. Xie, K.E. deKrafft, W. Lin, Doping Metal-Organic Frameworks for Water Oxidation, Carbon Dioxide Reduction, and Organic Photocatalysis, *J. Am. Chem. Soc.* 133 (2011) 13445-13454, <https://doi.org/10.1021/ja203564w>.
- [51] C. Wang, Z. Xie, K.E. deKrafft, W. Lin, Light-Harvesting Cross-Linked Polymers for Efficient Heterogeneous Photocatalysis, *ACS Appl. Mater. Interfaces* 4 (2012) 2288-2294, <https://doi.org/10.1021/am3003445>.
- [52] J.-L. Wang, C. Wang, K.E. deKrafft, W. Lin, Cross-linked Polymers with Exceptionally High Ru(bipy)₃²⁺ Loadings for Efficient Heterogeneous Photocatalysis, *ACS Catal.* 2 (2012) 417-424, <https://doi.org/10.1021/cs300027n>.
- [53] S. Li, L. Li, Y. Li, L. Dai, C. Liu, Y. Liu, J. Li, J. Lv, P. Li, B. Wang, Fully Conjugated Donor–Acceptor Covalent Organic Frameworks for Photocatalytic Oxidative Amine Coupling and Thioamide Cyclization, *ACS Catal.* 10 (2020) 8717-8726, <https://doi.org/10.1021/acscatal.0c01242>.
- [54] X. Lan, X. Liu, Y. Zhang, Q. Li, J. Wang, Q. Zhang, G. Bai, Unveiling Charge Dynamics in Acetylene-Bridged Donor– π –Acceptor Covalent Triazine Framework for Enhanced Photoredox Catalysis, *ACS Catal.* 11 (2021) 7429-7441, <https://doi.org/10.1021/acscatal.1c01794>.
- [55] J.-Y. Li, Y.-H. Li, M.-Y. Qi, Q. Lin, Z.-R. Tang, Y.-J. Xu, Selective Organic Transformations over Cadmium Sulfide-Based Photocatalysts, *ACS Catal.* 10 (2020) 6262-6280, <https://doi.org/10.1021/acscatal.0c01567>.
- [56] M.-Y. Qi, M. Conte, M. Anpo, Z.-R. Tang, Y.-J. Xu, Cooperative Coupling of Oxidative Organic Synthesis and Hydrogen Production over Semiconductor-Based Photocatalysts, *Chem. Rev.* 121 (2021) 13051-13085, <https://doi.org/10.1021/acs.chemrev.1c00197>.
- [57] M.-Y. Qi, M. Conte, Z.-R. Tang, Y.-J. Xu, Engineering Semiconductor Quantum Dots for Selectivity Switch on High-Performance Heterogeneous Coupling Photosynthesis, *ACS Nano* 16 (2022) 17444-17453, <https://doi.org/10.1021/acsnano.2c08652>.
- [58] M.-Y. Qi, Z.-R. Tang, Y.-J. Xu, Near Field Scattering Optical Model-Based Catalyst Design for Artificial Photoredox Transformation, *ACS Catal.* 13 (2023) 3971–3982, <https://doi.org/10.1021/acscatal.2c06397>.
- [59] A.G. Condie, J.C. González-Gómez, C.R.J. Stephenson, Visible-Light Photoredox Catalysis: Aza-Henry Reactions via C–H Functionalization, *J. Am. Chem. Soc.* 132 (2010) 1464-1465, <https://doi.org/10.1021/ja909145y>.

-
- [60] Z. Xie, C. Wang, K.E. deKrafft, W. Lin, Highly Stable and Porous Cross-Linked Polymers for Efficient Photocatalysis, *J. Am. Chem. Soc.* 133 (2011) 2056-2059 <https://doi.org/10.1021/ja109166b>.
- [61] C.-A. Wang, Y.-F. Han, K. Nie, Y.-W. Li, Porous organic frameworks with mesopores and [Ru(bpy)₃]²⁺ ligand built-in as a highly efficient visible-light heterogeneous photocatalyst, *Mater. Chem. Front.* 3 (2019) 1909-1917. <https://doi.org/10.1039/c9qm00316a>.
- [62] Y. Zhi, S. Ma, H. Xia, Y. Zhang, Z. Shi, Y. Mu, X. Liu, Construction of donor-acceptor type conjugated microporous polymers: A fascinating strategy for the development of efficient heterogeneous photocatalysts in organic synthesis, *Appl. Catal. B* 244 (2019) 36-44, <https://doi.org/10.1016/j.apcatb.2018.11.032>.
- [63] J. Chen, J. Cen, X. Xu, X. Li, The application of heterogeneous visible light photocatalysts in organic synthesis, *Catal. Sci. Technol.* 6 (2016) 349-362, <https://doi.org/10.1039/C5CY01289A>.
- [64] P.A. Lay, A.M. Sargeson, H. Taube, M.H. Chou, C. Creutz, *Cis*-Bis(2,2'-Bipyridine-N,N') Complexes of Ruthenium (III)/(II) and Osmium(III)/(II), *Inorg. Synth.* 24 (1986) 291-299, <https://doi.org/10.1002/9780470132555.ch78>.
- [65] Y. Huang, Q. Lin, J. Wu, N. Fu, Design and synthesis of a squaraine based near-infrared fluorescent probe for the ratiometric detection of Zn²⁺ ions, *Dyes Pigm.* 99 (2013) 699-704, <https://doi.org/10.1016/j.dyepig.2013.06.020>.
- [66] E.C. Constable, E. Figgemeier, C.E. Housecroft, J. Olsson, Y.C. Zimmermann, Electrochemical probing of ground state electronic interactions in polynuclear complexes of a new heteroditopic ligand, *Dalton Trans.* (2004), 1918-1927, <https://doi.org/10.1039/B404602A>.
- [67] F.Y. Kwong, A. Klapars, S.L. Buchwald, Copper-catalyzed coupling of alkylamines and aryl iodides: An efficient system even in an air atmosphere, *Org. Lett.* 4 (2002) 581-584, <https://doi.org/10.1021/ol0171867>.
- [68] P. Ma, Y. Liu, L. Chen, X. Zhao, B. Yang, J. Zhang, Photocatalyst-and additive-free decarboxylative alkylation of N-aryl tetrahydroisoquinolines induced by visible light. *Org. Chem. Front.* 8 (2021) 2473-2479, <https://doi.org/10.1039/D1QO00261A>.
- [69] K. Albert, B. Pfeleiderer, E. Bayer, R. Schnabel, Characterization of chemically modified glass surfaces by ¹³C and ²⁹Si CP/MAS NMR spectroscopy, *J. Colloid Interface Sci.* 142 (1991) 35-40, [https://doi.org/10.1016/0021-9797\(91\)90031-3](https://doi.org/10.1016/0021-9797(91)90031-3).

-
- [70] P. Vejayakumaran, I.A. Rahman, C.S. Sipaut, J. Ismail, C.K. Chee, Structural and thermal characterizations of silica nanoparticles grafted with pendant maleimide and epoxide groups, *J. Colloid Interface Sci.* 328 (2008) 81-91, <https://doi.org/10.1016/j.jcis.2008.08.054>.
- [71] J. Balcerzak, W. Redzynia, J. Tyczkowski, In-situ XPS analysis of oxidized and reduced plasma deposited ruthenium-based thin catalytic films, *Appl. Surf. Sci.* 426 (2017) 852-855, <https://doi.org/10.1016/j.apsusc.2017.07.248>.
- [72] S.F. Martin, Recent applications of imines as key intermediates in the synthesis of alkaloids and novel nitrogen heterocycles. *Pure Appl. Chem.* 81 (2009) 195-204, <http://dx.doi.org/10.1351/PAC-CON-08-07-03>.
- [73] J. Iwanejko, E. Wojaczyńska, Cyclic imines—preparation and application in synthesis. *Org. Biomol. Chem.* 16 (2018) 7296-7314, <https://doi.org/10.1039/C8OB01874J>.
- [74] S. Hübner, J.G. de Vries, V. Farina, Why Does Industry Not Use Immobilized Transition Metal Complexes as Catalysts? *Adv. Synth. Catal.* 358 (2016) 3-25, <http://doi.org/10.1002/adsc.201500846>.
- [75] For plausible photocatalytic mechanisms for the oxidative homocoupling of benzylamines under aerobic conditions, see references 53 and 54.
- [76] For plausible photocatalytic mechanisms for the aerobic C-H functionalization of N-phenyl-tetrahydroisoquinoline, see references 59 and 62.